Generation and complete analysis of the hyperentangled Bell state for photons assisted by quantum-dot spins in optical microcavities

Tie-Jun Wang,[1] Yao Lu,[1] and Gui Lu Long[1,2,*]

[1]*State Key Laboratory of Low-Dimensional Quantum Physics and Department of Physics, Tsinghua University, Beijing 100084, China*

[2]*Tsinghua National Laboratory for Information Science and Technology, Beijing 100084, China*

(Received 9 September 2012; published 31 October 2012)

We propose a scheme for the production of hyperentangled photon pairs as well as for the complete differentiation of 16 hyperentangled Bell states in both polarization and spatial-mode degrees of freedom using the quantum-dot cavity systems. This hyperentangled-Bell-state photon generation and the complete hyperentangled-Bell-state-analysis device can serve as crucial components of the high-capacity, long-distance quantum communication. We use the hyperentanglement quantum repeater as an example to show the application of this device. When the hyperentanglement quantum repeater operation is complete, two parties that are far from each other in quantum communication can share two Bell-state spin pairs simultaneously. By using numerical calculations we prove that the present scheme can both work in the weak- and strong-coupling regimes with current technology.

DOI: 10.1103/PhysRevA.86.042337 PACS number(s): 03.67.Hk, 03.67.Mn, 03.65.Ud, 42.50.Pq

I. INTRODUCTION

As a key quantum resource, entanglement plays a critical role in various quantum information processing protocols, such as the one-way quantum computer [1], quantum teleportation [2], dense coding [3], and some important quantum cryptographic schemes [4]. Hyperentanglement [5]—the entanglement of photon pairs simultaneously existing in more than one degree of freedom (DOF)—has been implemented in optical systems [6] in polarization-frequency DOFs [7], polarization-momentum DOFs [8], polarization-time-bin DOFs [9], and polarization-orbital-angular momentum DOFs [10]. In 2009, Vallone *et al.* [11] reported their experiment with a six-qubit hyperentangled state in three DOFs. The applications of hyperentanglement has been extensively studied for it can improve the channel capacity of long-distance quantum communications and can offer significant advantages in quantum communication protocols. For example, hyperentanglement is used for secure superdense coding [12], quantum error-correcting code [13], quantum cryptography [14], quantum repeater [15,16], and deterministic entanglement purification [17]. Furthermore, one of the most important applications of hyperentanglement at present is in the complete local Bell-state analysis. The complete and deterministic analysis of the two-photon Bell state (also called the Bell-state analysis) is required as a critical element for many important applications in quantum communication, such as quantum teleporation [2,18,19], quantum dense coding [3], quantum superdense coding [20], and so on. The unambiguous differentiation of the four Bell states that are encoded in polarization DOF is impossible when only linear optics is used [21]. However, one can manage to do so with the help of the hyperentanglement photons. In 2003, Walborn *et al.* [21] proposed a simple linear-optical scheme for the complete Bell-state measurement of photons by using hyperentanglement. In 2006, Carsten Schuck *et al.* [22] deterministically distinguished all four polarization Bell states of entangled photon pairs with the aid of polarization-time-bin hyperentanglement in an experiment. In 2007, Barbieri *et al.* [23] realized a complete and deterministic Bell-state measurement using linear optics and two-photon polarization-momentum hyperentanglement in experiment.

A quantum system with two photons hyperentangled in polarization and spatial-mode DOFs has 16 generalized Bell states which can be expressed as

$$|\varphi^{AB}\rangle_{PS} = |\zeta_{AB}\rangle_P \otimes |\eta_{AB}\rangle_S, \tag{1}$$

where subscripts A and B represent the two photons in the hyperentangled state. The subscript P denotes the polarization DOF, and $|\zeta_{AB}\rangle_P$ is one of the four Bell states in the polarization DOF, which is expressed as

$$\begin{aligned} |\phi^{\pm}_{AB}\rangle_P &= \frac{1}{\sqrt{2}}(|RR\rangle_{AB} \pm |LL\rangle_{AB}), \\ |\psi^{\pm}_{AB}\rangle_P &= \frac{1}{\sqrt{2}}(|RL\rangle_{AB} \pm |LR\rangle_{AB}). \end{aligned} \tag{2}$$

Here $|L\rangle$ and $|R\rangle$ represent the left and right circular polarizations of photons, respectively. The subscript S denotes the spatial-mode DOF, and $|\eta_{AB}\rangle_S$ is one of the four Bell states in the spatial-mode DOF, which is expressed as

$$\begin{aligned} |\phi^{\pm}_{AB}\rangle_S &= \frac{1}{\sqrt{2}}(|a_1b_1\rangle_{AB} \pm |a_2b_2\rangle_{AB}), \\ |\psi^{\pm}_{AB}\rangle_S &= \frac{1}{\sqrt{2}}(|a_1b_2\rangle_{AB} \pm |a_2b_1\rangle_{AB}), \end{aligned} \tag{3}$$

where $a_1(b_1)$ and $a_2(b_2)$ are the different spatial modes for the photon $A(B)$. This type of hyperentangled-photon pairs can be produced by using the parametric down-conversion techniques in nonlinear crystals such as β-barium-borate (BBO) [24]. However, some shortcomings of this method, such as low quantum efficiencies and high multiphoton generation probabilities, can limit its applications in quantum information processing. In addition, it has been proven that, only with

*gllong@tsinghua.edu.cn

the help of linear optics, one can distinguish 7 states in the group of 16 orthogonal hyperentangled Bell states in two degrees of freedom, and the upper bound of the maximal number of mutually distinguishable n-qubit Bell-like states is $2^{n+1}-1$, which is true for $n=1$ and $n=2$ [25]. In 2010, Sheng *et al.* [26] proposed a scheme to distinguish the 16 hyperentangled Bell states completely with the help of cross-Kerr nonlinearity and discussed the application of this scheme in quantum teleportation and entanglement swapping. Although the cross-Kerr nonlinearity in the optical single-photon regime has been widely used, it remains a controversial assumption without the current technical supports [27,28].

Quantum dot [29] is one of the best candidates to generate the single photons [30], entangled photon pairs [31], and hyperentangled photon pairs [32], because of its high quantum efficiency, single-photon characteristics, and high stability. Moreover, it is comparatively easy to embed the QDs in the solid-state cavities. The deterministic transfer of quantum information between photons and spins in QDs can be promoted by the structure of a cavity-QD system. In a weak-coupling cavity where the vacuum Rabi frequency is less than the cavity decay rate, the electron-spin-cavity system works like a beam splitter in the limit of a weak incoming field [33]. In 2006, Waks and Vuckovic proposed a quantum repeater scheme by using the interaction of a cavity and a dipole in a weak-coupling regime [34]. Afterward, this spin-photon interface has been widely used in studies on universal gates [35–37], deterministic optical quantum computing [38], photon entanglement generation [37,39], hybrid entanglement generation [39], quantum purification and concentration [40], the Bell-state analysis [41], and its various application in quantum communication processing such as teleportation and entanglement swapping.

Based on these studies, we exploit the function of the double-sided cavity as a SWAP gate between the polarization DOF and the spatial-mode DOF of photons and propose a scheme that can be used as a hyperentangled-Bell-state photon generation (HBSG) source as well as a complete hyperentangled-Bell-state analyzer (HBSA). This HBSG and HBSA device can be used for high-capacity teleportation and entanglement swapping which are crucial components of long-distance quantum communication. Here we use a hyperentanglement quantum repeater as an example to illustrate the application of this device. In the normal quantum repeater proposals which use the photon pairs entangled in only one DOF, the long-distance-transmission line is divided into some segments with a shorter length in which the loss is largely diminished, and after one complete quantum repeater operation, in principle, the two parties that are far from each other in quantum communication can share only one entangled pair stored in the quantum-state memory units. However, by using hyperentangled photon pairs, the transmission capacity of the channels is increased, and after one complete hyperentanglement quantum repeater operation, the two parties theoretically can share two entangled spin pairs simultaneously. By using numerical calculations we demonstrate that the present scheme does not require the high cavity limit, and that it can work in the weak- and strong-coupling regime using current technology.

II. GENERATION OF HYPERENTANGLED BELL STATES BASED ON QUANTUM-DOT SPIN AND OPTICAL MICROCAVITY SYSTEM

Here we consider a singly charged QD that is embedded in a double-sided optical microcavity with the partially reflective top and bottom mirrors, as shown in Fig. 1. An exciton consisting of two electrons bound to one hole with negative charges can be created by the optical excitation of a photon and an electron spin. If the photon is in the state $|R^{\uparrow}\rangle$ or $|L^{\downarrow}\rangle$ ($s_z=1$), it only couples with the electron that is in the state $|\uparrow\rangle$ ($J_z=+\frac{1}{2}$) to the exciton state $|\uparrow\downarrow\Uparrow\rangle$; otherwise, when the photon is in the state $|R^{\downarrow}\rangle$ or $|L^{\uparrow}\rangle$, it couples the electron in the spin state $|\downarrow\rangle$ ($J_z=-\frac{1}{2}$) to the exciton state $|\downarrow\uparrow\Downarrow\rangle$. Here $|\Uparrow\rangle$ and $|\Downarrow\rangle$ represent heavy-hole spin states with $J_z=\frac{3}{2}$ and $J_z=-\frac{3}{2}$, respectively. This dipole interaction leads to the giant circular birefringence (GCB) in both strongly coupling and weakly coupling regimes [39]. GCB manifests as different reflection and transmission coefficients between the $|L\rangle$ and $|R\rangle$ photons. All reflection and transmission coefficients of this spin-cavity system can be determined by solving the Heisenberg equations of motion for the cavity-field operator ($\hat{a}$) and the exciton X^- dipole operator (σ_-) in weak excitation approximation [35–37,39]

$$\begin{aligned}\frac{d\hat{a}}{dt} &= -\left[i(\omega_c-\omega)+\kappa+\frac{\kappa_s}{2}\right]\hat{a}-g\sigma_- \\ &\quad -\sqrt{\kappa}\hat{a}_{\mathrm{in}'}-\sqrt{\kappa}\hat{a}_{\mathrm{in}}+\hat{H}, \\ \frac{d\sigma_-}{dt} &= -\left[i(\omega_{X^-}-\omega)+\frac{\gamma}{2}\right]\sigma_- - g\sigma_z\hat{a}+\hat{G}, \\ \hat{a}_r &= \hat{a}_{\mathrm{in}}+\sqrt{\kappa}\hat{a}, \quad \hat{a}_t = \hat{a}_{\mathrm{in}'}+\sqrt{\kappa}\hat{a},\end{aligned} \tag{4}$$

where ω, ω_c, and ω_{X^-} are the frequencies of the photon, the cavity, and X^- transition, respectively; g represents the coupling constant; γ is the exciton dipole decay rate; and κ and κ_s are the cavity decay rate and the leaky rate, respectively. $\hat{H}$ and $\hat{G}$ are the noise operators related to reservoirs. $\hat{a}_{\mathrm{in}}$, $\hat{a}_{\mathrm{in}'}$ and $\hat{a}_r$, $\hat{a}_t$ are the input and output field operators. For a double-sided optical microcavity system [33,39], the reflection r_h and transmission t_h coefficient in a coupled cavity in the resonant interaction case can be described by

$$\begin{aligned}r_h(\omega) &= 1+t_h(\omega), \\ t_h(\omega) &= -\frac{\kappa\left[i(\omega_{X^-}-\omega)+\frac{\gamma}{2}\right]}{\left[i(\omega_{X^-}-\omega)+\frac{\gamma}{2}\right]\left[i(\omega_c-\omega)+\kappa+\frac{\kappa_s}{2}\right]+g^2}.\end{aligned} \tag{5}$$

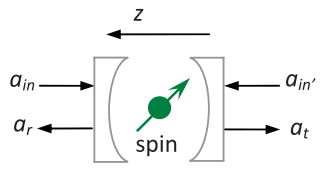

FIG. 1. (Color online) A charged quantum dot (QD) inside a micropillar microcavity with a circular cross section in a double-sided cavity. Here L and R represent the left circular polarization $|L\rangle$ and the right circular polarization $|R\rangle$ of photons, respectively.

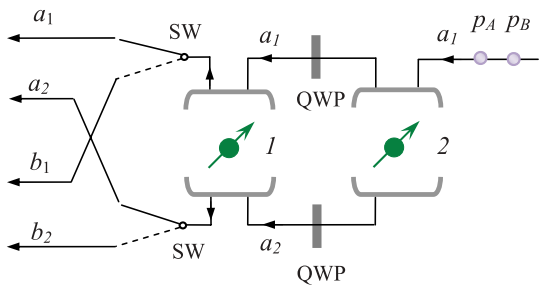

FIG. 2. (Color online) Schematic diagram of a hyperentangled Bell-state photon-generation (HBSG) source. QWP represents a quarter-wave plate which can be used to accomplish the Hadamard operation on the $|R\rangle$ and $|L\rangle$ polarized states.

When $g = 0$, the reflection r_0 and transmission t_0 coefficients in an uncoupled cavity are

$$r_0(\omega) = \frac{i(\omega_0 - \omega) + \frac{\kappa_s}{2}}{i(\omega_c - \omega) + \kappa + \frac{\kappa_s}{2}}, \qquad t_0(\omega) = \frac{-\kappa}{i(\omega_0 - \omega) + \kappa + \frac{\kappa_s}{2}}. \tag{6}$$

Thus when the side leakage and cavity loss (k_s) can be ignored, in the resonant interaction case, the cold (uncoupled) and hot (coupled) cavities generally have different reflection and transmission coefficients, and the dynamics of the photon and of the spin in the cavity are described as follows:

$$\begin{aligned}
&|R^{\uparrow},\uparrow\rangle \to |L^{\downarrow},\uparrow\rangle, \quad && |L^{\uparrow},\uparrow\rangle \to -|L^{\uparrow},\uparrow\rangle,\\
&|R^{\downarrow},\uparrow\rangle \to -|R^{\downarrow},\uparrow\rangle, \quad && |L^{\downarrow},\uparrow\rangle \to |R^{\uparrow},\uparrow\rangle,\\
&|R^{\uparrow},\downarrow\rangle \to -|R^{\uparrow},\downarrow\rangle, \quad && |L^{\uparrow},\downarrow\rangle \to |R^{\downarrow},\downarrow\rangle,\\
&|R^{\downarrow},\downarrow\rangle \to |L^{\uparrow},\downarrow\rangle, \quad && |L^{\downarrow},\downarrow\rangle \to -|L^{\downarrow},\downarrow\rangle.
\end{aligned} \tag{7}$$

Here the superscript arrows $\uparrow$ and $\downarrow$ in the photon state indicate the propagation direction along the z axis. Thus the photon polarization and electron spin may become entangled when this spin-cavity unit is used. In this paper we use this spin-cavity unit to construct a device consisting of an HBSG source and a complete HBSA for high-capacity, long-distance quantum communication.

The principles of HBSG are shown in Fig. 2. Two photons p_A and p_B are prepared in the same initial state $|\varphi_{p1}\rangle = |\varphi_{p2}\rangle = |R\rangle$, and the two spins (1 and 2) are prepared in the state $|+\rangle_1 = |+\rangle_2 = \frac{1}{\sqrt{2}}(|\uparrow\rangle + |\downarrow\rangle)$. The quarter-wave plates (QWPs) in Fig. 2 are used to complete the Hadamard operation in the polarization DOF on a single photon. That is,

$$|R\rangle \xleftrightarrow{\text{QWP}} (|R\rangle + |L\rangle)/\sqrt{2}, \quad |L\rangle \xleftrightarrow{\text{QWP}} (|R\rangle - |L\rangle)/\sqrt{2}. \tag{8}$$

Figure 2 shows that photons p_A and p_B are successively sent into the cavities from the right input port of the HBSG device. After passing through two cavities, the photons can be entangled with the electron spins. The evolution of the entire system can then be described as

$$\begin{aligned}
&|\varphi_{p_A}\rangle|\varphi_{p_B}\rangle|+\rangle_1|+\rangle_2\\
&\xrightarrow{\text{cavity2}} \tfrac{1}{2}|+\rangle_1(|\phi^+_{AB}\rangle_P|\phi^+_{AB}\rangle_S|+\rangle_2 + |\phi^+_{AB}\rangle_P|\phi^-_{AB}\rangle_S|-\rangle_2\\
&\quad - |\phi^-_{AB}\rangle_P|\phi^+_{AB}\rangle_S|-\rangle_2 - |\phi^-_{AB}\rangle_P|\phi^-_{AB}\rangle_S|+\rangle_2)\\
&\xrightarrow{\text{QWP}} \tfrac{1}{2}|+\rangle_1(|\phi^+_{AB}\rangle_P|\phi^+_{AB}\rangle_S|+\rangle_2 + |\phi^+_{AB}\rangle_P|\phi^-_{AB}\rangle_S|-\rangle_2\\
&\quad - |\psi^+_{AB}\rangle_P|\phi^+_{AB}\rangle_S|-\rangle_2 - |\psi^+_{AB}\rangle_P|\phi^-_{AB}\rangle_S|+\rangle_2)\\
&\xrightarrow{\text{cavity1}} \tfrac{1}{2}(|\phi^+_{AB}\rangle_P|\phi^+_{AB}\rangle_S|+\rangle_1|+\rangle_2 + |\phi^-_{AB}\rangle_P|\phi^+_{AB}\rangle_S|-\rangle_1|-\rangle_2\\
&\quad + |\phi^+_{AB}\rangle_P|\psi^+_{AB}\rangle_S|+\rangle_1|-\rangle_2 + |\phi^-_{AB}\rangle_P|\psi^+_{AB}\rangle_S|-\rangle_1|+\rangle_2),
\end{aligned} \tag{9}$$

where $|\pm\rangle = \frac{1}{\sqrt{2}}(|\uparrow\rangle \pm |\downarrow\rangle)$.

Equation (9) shows that when the photons pass through a double-sided cavity, the states in the polarization DOF and the states in the spatial-mode DOF of the two photons A and B are interchangeable. In other words, the double-sided cavity works as a SWAP gate for these two DOFs. At the same time, the spin in the cavity records the relationship between the phase information in these two DOFs. If the phase information in the two DOFs are the same (i.e., the hyperentangled state is either one of $|\phi^+_{AB}\rangle_P|\phi^+_{AB}\rangle_S, |\phi^-_{AB}\rangle_P|\phi^-_{AB}\rangle_S, |\psi^+_{AB}\rangle_P|\phi^+_{AB}\rangle_S$, and $|\psi^-_{AB}\rangle_P|\phi^-_{AB}\rangle_S$), then the spin remains in the state $|+\rangle$ when the two photons AB pass through the cavity. Otherwise, the state of the spin changes to $|-\rangle$ when the phase information in the two DOFs differ (the hyperentangled state is either one of $|\phi^+_{AB}\rangle_P|\phi^-_{AB}\rangle_S, |\phi^-_{AB}\rangle_P|\phi^+_{AB}\rangle_S, |\psi^+_{AB}\rangle_P|\phi^-_{AB}\rangle_S$, and $|\psi^-_{AB}\rangle_P|\phi^+_{AB}\rangle_S$). Therefore, the spin states divide the states of the AB photons into two groups: $\{|\zeta^{\pm}_{AB}\rangle_P|\eta^{\pm}_{AB}\rangle_S, |\zeta^{\pm}_{AB}\rangle_P|\eta^{\mp}_{AB}\rangle_S\}$. After the QWPs, $|\phi^-_{AB}\rangle_P$ becomes $|\psi^+_{AB}\rangle_P$, whereas $|\phi^+_{AB}\rangle_P$ remains unchanged. The state of the two photons (A and B) can be determined using the outcomes of the two spins (1 and 2). The relationship between the measurement outcomes of the two spins and the hyperentangled states of the two-photon system AB is shown in Table I.

TABLE I. The relation between the outcomes of the states of the two spins and the obtained final hyperentangled state.

Spin 1 and 2	Hyperentangled state
$\|+\rangle_1\|+\rangle_2$	$\|\phi^+_{AB}\rangle_P \otimes \|\phi^+_{AB}\rangle_S$
$\|-\rangle_1\|-\rangle_2$	$\|\phi^-_{AB}\rangle_P \otimes \|\phi^+_{AB}\rangle_S$
$\|+\rangle_1\|-\rangle_2$	$\|\phi^+_{AB}\rangle_P \otimes \|\psi^+_{AB}\rangle_S$
$\|-\rangle_1\|+\rangle_2$	$\|\phi^-_{AB}\rangle_P \otimes \|\psi^+_{AB}\rangle_S$

Table I shows that if the spins 1 and 2 are in an even-parity state $|+\rangle_1|+\rangle_2$ (or $|-\rangle_1|-\rangle_2$), the two photons A and B are in the hyperentangled Bell state $|\phi^+_{AB}\rangle_P|\phi^+_{AB}\rangle_S$ (or $|\phi^-_{AB}\rangle_P|\psi^-_{AB}\rangle_S$). Otherwise, when the 12 spins are in the odd-parity state $|+\rangle_1|-\rangle_2$ (or $|-\rangle_1|+\rangle_2$), the two photons AB are in the hyperentangled Bell state $|\psi^+_{AB}\rangle_P|\phi^-_{AB}\rangle_S$ (or $|\phi^+_{AB}\rangle_P|\phi^-_{AB}\rangle_S$). By measuring the two-electron spins 1 and 2 using the spin basis $\{|+\rangle, |-\rangle\}$ [36,37], one can determine the hyperentangled states of the two photons. By far we have described the scheme of our HBSG in the linear regime of the QD-double-sided-cavity systems.

III. THE COMPLETE HYPERENTANGLED BELL-STATES ANALYSIS BASED ON QUANTUM-DOT SPIN AND OPTICAL MICROCAVITY SYSTEM

Another application of this device is to complete the 16 hyperentangled Bell-state analysis (see Fig. 3). Let us discuss the 16 cases one by one. Consider that the hyperentangled

photon pair AB is in one of the 16 hyperentangled Bell states that forms in Eq. (1). Electron spins 1 and 2 are both initialized in the state $|\Psi^s\rangle_i = (|\uparrow\rangle + |\downarrow\rangle)_i/\sqrt{2}$, where $i = 1,2$. First, let photon A pass through the cavities from the left input port, followed by photon B. A time interval $\triangle t$ exists between photons A and B. Initially, an optical switch directs photon A from Alice to the system until it is detected in H_D or V_D as shown in Fig. 3. The switch is then switched to await the detection of photon B. $\triangle t$ should be less than the spin coherence time T.

According to the evolution rules of the photon and the spin in the cavity described in Eq. (7), after the photons passes through the cavities and the HWPs, the whole system of the two photons and the two spins evolves as

$$
\begin{aligned}
&|\phi^+_{AB}\rangle_P(|\psi^+_{AB}\rangle_P)|\phi^+_{AB}\rangle_S \xrightarrow{|+\rangle^s_1|+\rangle^s_2} |\phi^+_{AB}\rangle_P(|\psi^+_{AB}\rangle_P)|\phi^+_{AB}\rangle_S|+\rangle^s_1|+\rangle^s_2,\\
&|\phi^+_{AB}\rangle_P(|\psi^+_{AB}\rangle_P)|\phi^-_{AB}\rangle_S \xrightarrow{|+\rangle^s_1|+\rangle^s_2} |\phi^+_{AB}\rangle_P(|\psi^+_{AB}\rangle_P)|\psi^+_{AB}\rangle_S|-\rangle^s_1|+\rangle^s_2,\\
&|\phi^-_{AB}\rangle_P(|\psi^-_{AB}\rangle_P)|\phi^+_{AB}\rangle_S \xrightarrow{|+\rangle^s_1|+\rangle^s_2} |\phi^-_{AB}\rangle_P(|\psi^-_{AB}\rangle_P)|\phi^+_{AB}\rangle_S|-\rangle^s_1|-\rangle^s_2,\\
&|\phi^-_{AB}\rangle_P(|\psi^-_{AB}\rangle_P)|\phi^-_{AB}\rangle_S \xrightarrow{|+\rangle^s_1|+\rangle^s_2} |\phi^-_{AB}\rangle_P(|\psi^-_{AB}\rangle_P)|\psi^+_{AB}\rangle_S|+\rangle^s_1|-\rangle^s_2,
\end{aligned}
$$

and

$$
\begin{aligned}
&|\psi^+_{AB}\rangle_P(|\phi^+_{AB}\rangle_P)|\psi^+_{AB}\rangle_S \xrightarrow{|+\rangle^s_1|+\rangle^s_2} |\psi^+_{AB}\rangle_P(|\phi^+_{AB}\rangle_P)|\phi^-_{AB}\rangle_S|+\rangle^s_1|-\rangle^s_2,\\
&|\psi^+_{AB}\rangle_P(|\phi^+_{AB}\rangle_P)|\psi^-_{AB}\rangle_S \xrightarrow{|+\rangle^s_1|+\rangle^s_2} |\psi^+_{AB}\rangle_P(|\phi^+_{AB}\rangle_P)|\psi^-_{AB}\rangle_S|-\rangle^s_1|-\rangle^s_2,\\
&|\psi^-_{AB}\rangle_P(|\phi^-_{AB}\rangle_P)|\psi^+_{AB}\rangle_S \xrightarrow{|+\rangle^s_1|+\rangle^s_2} |\psi^-_{AB}\rangle_P(|\phi^-_{AB}\rangle_P)|\phi^-_{AB}\rangle_S|-\rangle^s_1|+\rangle^s_2,\\
&|\psi^-_{AB}\rangle_P(|\phi^-_{AB}\rangle_P)|\psi^-_{AB}\rangle_S \xrightarrow{|+\rangle^s_1|+\rangle^s_2} |\psi^-_{AB}\rangle_P(|\phi^-_{AB}\rangle_P)|\psi^-_{AB}\rangle_S|+\rangle^s_1|+\rangle^s_2.
\end{aligned}
\tag{10}
$$

Photons A and B can be independently measured in both the polarization and the spatial-mode DOFs with single-photon detectors, and then the two-electron spins 1 and 2 be measured using the spin basis $\{|+\rangle,|-\rangle\}$. The relationship between the measurement outcomes of the states of the two photons AB and the two spins 12 and the initial hyperentangled states of the two-photon system AB is shown in Table II.

From Table II one can obtain the complete and deterministic analysis on quantum hyperentangled Bell states. The outcomes of two photon polarization states determine the parity information in the polarization DOF, whereas the outcomes of the spatial-mode states determines the phase information in the spatial-mode DOF. In detail, when the two photons are detected in an even-parity (odd-parity) state in the polarization DOF [i.e., $|RR\rangle_{AB}$ or $|LL\rangle_{AB}$ ($|RL\rangle_{AB}$ or $|LR\rangle_{AB}$)], the photons are initially in the even-parity (odd-parity) polarization state $|\phi^{\pm}\rangle_P$ ($|\psi^{\pm}\rangle_P$). When the two photons are detected in an even-parity (odd-parity) state in the spatial-mode DOF [i.e., $|a_1b_1\rangle_{AB}$ or $|a_2b_2\rangle_{AB}$ ($|a_1b_2\rangle_{AB}$ or $|a_2b_1\rangle_{AB}$)], the photons are initially in the spatial-mode state $|\phi^+\rangle_S$ or $|\psi^+\rangle_S$ ($|\phi^-\rangle_S$ or $|\psi^-\rangle_S$).

The spin 1 is used to record the relation of the phase information in the two DOFs. By using the correlated measurements

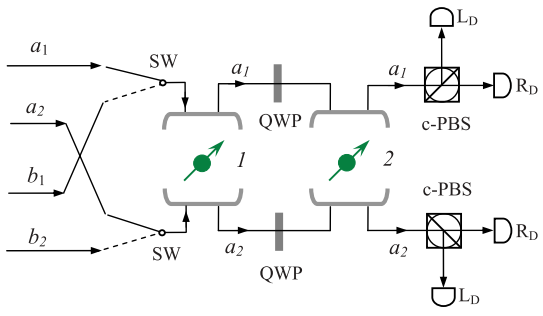

FIG. 3. (Color online) The schematic diagram of the hyperentangled Bell-state analyzer (HBSA). The c-PBS is a polarizing beam splitter in the circular basis which transmits the input right-circularly polarized photon $|R\rangle$ and reflects the left-circularly polarized photon $|L\rangle$. QWP represents a quarter-wave plate that can be used to accomplish the Hadamard operation on the $|R\rangle$ and $|L\rangle$ polarized states. R_D and L_D are two single-photon detectors.

TABLE II. Relationship between the measurement outcomes of the state of the whole spin-photon system and the initial hyperentangled Bell states.

Spin 1 and 2	Polarization	Spatial mode	$\|\varphi\rangle_{AB}$
$\|+\rangle_1\|+\rangle_2$	RR, LL	$\|a_1\rangle\|b_1\rangle, \|a_2\rangle\|b_2\rangle$	$\|\phi^+_{AB}\rangle_P \otimes \|\phi^+_{AB}\rangle_S$
$\|+\rangle_1\|+\rangle_2$	RL, LR	$\|a_1\rangle\|b_1\rangle, \|a_2\rangle\|b_2\rangle$	$\|\psi^+_{AB}\rangle_P \otimes \|\phi^+_{AB}\rangle_S$
$\|+\rangle_1\|+\rangle_2$	RL, LR	$\|a_1\rangle\|b_2\rangle, \|a_2\rangle\|b_1\rangle$	$\|\psi^-_{AB}\rangle_P \otimes \|\psi^-_{AB}\rangle_S$
$\|+\rangle_1\|+\rangle_2$	RR, LL	$\|a_1\rangle\|b_2\rangle, \|a_2\rangle\|b_1\rangle$	$\|\phi^-_{AB}\rangle_P \otimes \|\psi^-_{AB}\rangle_S$
$\|-\rangle_1\|-\rangle_2$	RR, LL	$\|a_1\rangle\|b_1\rangle, \|a_2\rangle\|b_2\rangle$	$\|\phi^-_{AB}\rangle_P \otimes \|\phi^+_{AB}\rangle_S$
$\|-\rangle_1\|-\rangle_2$	RL, RL	$\|a_1\rangle\|b_1\rangle, \|a_2\rangle\|b_2\rangle$	$\|\psi^-_{AB}\rangle_P \otimes \|\phi^+_{AB}\rangle_S$
$\|-\rangle_1\|-\rangle_2$	RL, LR	$\|a_1\rangle\|b_2\rangle, \|a_2\rangle\|b_1\rangle$	$\|\psi^+_{AB}\rangle_P \otimes \|\psi^-_{AB}\rangle_S$
$\|-\rangle_1\|-\rangle_2$	RR, LL	$\|a_1\rangle\|b_2\rangle, \|a_2\rangle\|b_1\rangle$	$\|\phi^+_{AB}\rangle_P \otimes \|\psi^-_{AB}\rangle_S$
$\|+\rangle_1\|-\rangle_2$	RR, LL	$\|a_1\rangle\|b_2\rangle, \|a_2\rangle\|b_1\rangle$	$\|\phi^-_{AB}\rangle_P \otimes \|\phi^+_{AB}\rangle_S$
$\|+\rangle_1\|-\rangle_2$	RL, LR	$\|a_1\rangle\|b_2\rangle, \|a_2\rangle\|b_1\rangle$	$\|\psi^-_{AB}\rangle_P \otimes \|\phi^-_{AB}\rangle_S$
$\|+\rangle_1\|-\rangle_2$	RL, LR	$\|a_1\rangle\|b_1\rangle, \|a_2\rangle\|b_2\rangle$	$\|\psi^+_{AB}\rangle_P \otimes \|\psi^+_{AB}\rangle_S$
$\|+\rangle_1\|-\rangle_2$	RR, LL	$\|a_1\rangle\|b_1\rangle, \|a_2\rangle\|b_2\rangle$	$\|\phi^+_{AB}\rangle_P \otimes \|\psi^+_{AB}\rangle_S$
$\|-\rangle_1\|+\rangle_2$	RR, LL	$\|a_1\rangle\|b_2\rangle, \|a_2\rangle\|b_1\rangle$	$\|\phi^+_{AB}\rangle_P \otimes \|\phi^-_{AB}\rangle_S$
$\|-\rangle_1\|+\rangle_2$	RL, RL	$\|a_1\rangle\|b_2\rangle, \|a_2\rangle\|b_1\rangle$	$\|\psi^+_{AB}\rangle_P \otimes \|\phi^-_{AB}\rangle_S$
$\|-\rangle_1\|+\rangle_2$	RL, LR	$\|a_1\rangle\|b_1\rangle, \|a_2\rangle\|b_2\rangle$	$\|\psi^-_{AB}\rangle_P \otimes \|\psi^+_{AB}\rangle_S$
$\|-\rangle_1\|+\rangle_2$	RR, LL	$\|a_1\rangle\|b_1\rangle, \|a_2\rangle\|b_2\rangle$	$\|\phi^-_{AB}\rangle_P \otimes \|\psi^+_{AB}\rangle_S$

on the photons with the spatial-mode basis $\{|a1\rangle,|a2\rangle\}$ and then measuring the electron spins 1 with the spin basis $\{|+\rangle,|-\rangle\}$, one can determine the phase information in polarization DOF of the initial two-photon states. When the phase information in these two DOFs are the same ($|\phi_{AB}^{\pm}\rangle_P|\phi_{AB}^{\pm}\rangle_S$, $|\psi_{AB}^{\pm}\rangle_P|\phi_{AB}^{\pm}\rangle_S$, $|\phi_{AB}^{\pm}\rangle_P|\psi_{AB}^{\pm}\rangle_S$, or $|\psi_{AB}^{\pm}\rangle_P|\psi_{AB}^{\pm}\rangle_S$), the electron-spin 1 is in the state $|+\rangle_1^s$. Otherwise, the electron-spin 1 is in the state $|-\rangle_1^s$ when the phase information in these two DOFs are different ($|\phi_{AB}^{\pm}\rangle_P|\phi_{AB}^{\mp}\rangle_S$, $|\psi_{AB}^{\pm}\rangle_P|\phi_{AB}^{\mp}\rangle_S$, $|\phi_{AB}^{\pm}\rangle_P|\psi_{AB}^{\mp}\rangle_S$, or $|\psi_{AB}^{\pm}\rangle_P|\psi_{AB}^{\mp}\rangle_S$). The phase information in polarization DOF can be obtained when the phase information in spatial-mode DOF is determined and spin 1 is measured using $\{|+\rangle,|-\rangle\}$ as the basis. Note that the states of the two DOFs will be swapped after the first cavity, that is, the spin-cavity unit acts as a SWAP gate for the two DOFs. Therefore, by using HWP, and cavity 2, the relationship between the phase information in the polarization DOF and the parity information in the spatial-mode DOF can be determined. In addition, by using the outcomes of the states of the photons AB in the polarization and spatial-mode DOFs and the measurements of the spins 1 and 2, the initial hyperentangled-Bell state of the two photons AB can be determined. This discussion shows that our device in Fig. 3 can theoretically accomplish the complete and deterministic HBSA with 100% success probability.

IV. APPLICATIONS OF HBSG AND HBSA IN QUANTUM COMMUNICATION

As the HBSG source and the complete and deterministic HBSA are important to quantum communication, it is interesting to discuss the applications of HBSG and HBSA. Here we use the hyperentanglement quantum repeater with the present spin-cavity device as an example and describe its working mechanism (see Fig. 4). A hyperentanglement quantum repeater enables two parties that are far from each other in quantum communication to simultaneously share more than one entangled-state pair without directly

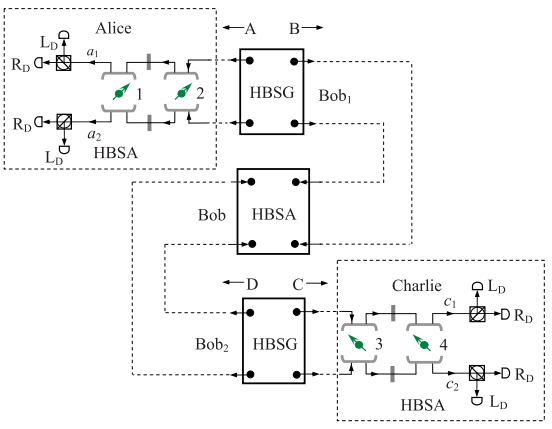

FIG. 4. (Color online) Schematic diagram of the hyperentanglement quantum repeater. The initial hyperentangled states are prepared in nodes Bob_1 and Bob_2 (including the four photons). After Bob performs the HBSA on the two photons BD, Alice and Charlie can obtain the hyperentangled state between the photons A and C. This hyperentangled photon pair can then be used to acquire the two entangled spin pairs simultaneously.

interacting with each other. In Fig. 4 we assume that the two hyperentangled Bell-state pairs AB and CD are generated by Bob_1 and Bob_2, respectively, and that these Bell-state pairs are in the same hyperentangled states: $|\phi_{AB(CD)}^{+}\rangle_P|\phi_{AB(CD)}^{+}\rangle_S$. Bob_1 sends photon A to Alice and sends photon B to Bob. Bob_2 sends photon C to Charlie but sends photon D to Bob. The task of Bob is to perform the hyperentanglement-swapping operation and entangle the two photons A and C in both the polarization and the spatial-mode DOFs. As shown in Fig. 3, Bob sends two photons B and D into the left input port of the HBSA devices successively, and then detects them at the right export in both the polarization and the spatial-mode DOFs, and finally completes entanglement swapping of hyperentangled states by measuring the two QDs in his hand in basis $\{|+\rangle,|-\rangle\}$. The state of the whole system can be rewritten as

$$\begin{aligned}
&|\phi_{AB}^{+}\rangle_P|\phi_{CD}^{+}\rangle_P\otimes|\phi_{AB}^{+}\rangle_S|\phi_{CD}^{+}\rangle_S\\
&\quad\rightarrow\tfrac{1}{4}(|\phi_{AC}^{+}\rangle_P|\phi_{BD}^{+}\rangle_P+|\phi_{AC}^{-}\rangle_P|\phi_{BD}^{-}\rangle_P+|\psi_{AC}^{+}\rangle_P|\psi_{BD}^{+}\rangle_P\\
&\qquad+|\psi_{AC}^{-}\rangle_P|\psi_{BD}^{-}\rangle_P)\otimes(|\phi_{AC}^{+}\rangle_S|\phi_{BD}^{+}\rangle_S+|\phi_{AC}^{-}\rangle_S|\phi_{BD}^{-}\rangle_S\\
&\qquad+|\psi_{AC}^{+}\rangle_S|\psi_{BD}^{+}\rangle_S+|\psi_{AC}^{-}\rangle_S|\psi_{BD}^{-}\rangle_S).
\end{aligned}\tag{11}$$

If the outcome of HBSA is $|\phi_{BD}^{+}\rangle_P|\phi_{BD}^{+}\rangle_S$, the two photons held by Alice and Charlie are in the hyperentangled state $|\phi_{AC}^{+}\rangle_P|\phi_{AC}^{+}\rangle_S$. Alice and Charlie each have a HBSA device. Alice sends her photon A into the HBSA devices and detects it after the two cavities. Charlie performs the same operation on his photon C. The state of the whole system, which consists of the photons AC and the four electron spins 1234, evolves into the following state:

$$\begin{aligned}
&[|RR\rangle_{AC}+|LL\rangle_{AC}]\otimes[(|a_1c_1\rangle_{AC}+|a_2c_2\rangle_{AC})|\phi^{+}\rangle_{23}|\phi^{+}\rangle_{14}\\
&\quad+(|a_1c_2\rangle_{AC}-|a_2c_1\rangle_{AC})|\psi^{+}\rangle_{23}|\psi^{-}\rangle_{14}]\\
&\quad+[|RL\rangle_{AC}+|LR\rangle_{AC}]\otimes[(|a_1c_2\rangle_{AC}\\
&\quad+|a_2c_1\rangle_{AC})|\phi^{+}\rangle_{23}|\psi^{+}\rangle_{14}\\
&\quad-(|a_1c_1\rangle_{AC}-|a_2c_2\rangle_{AC})|\psi^{+}\rangle_{23}|\phi^{-}\rangle_{14}],
\end{aligned}\tag{12}$$

where

$$\begin{aligned}
|\phi^{\pm}\rangle_{ij}&=\frac{1}{\sqrt{2}}(|\uparrow\uparrow\rangle\pm|\downarrow\downarrow\rangle)_{ij},\\
|\psi^{\pm}\rangle_{ij}&=\frac{1}{\sqrt{2}}(|\uparrow\downarrow\rangle\pm|\downarrow\uparrow\rangle)_{ij}.
\end{aligned}\tag{13}$$

Here $i=2,1$ and $j=3,4$. If the outcomes of HBSA lead to the other 15 hyperentangled Bell states, as is shown in Eq. (1), Alice and Charlie can, in principle, easily transform these Bell states into $|\phi_{BD}^{+}\rangle_P|\phi_{BD}^{+}\rangle_S$ using linear optics.

Equation (12) shows that after the whole hyperentanglement quantum repeater operation [42], Alice and Charlie can simultaneously obtain two maximally entangled spin pairs 23 and 14 in the $|\phi^{+}\rangle_{23}$ and $|\phi^{+}\rangle_{14}$ states with or without a single-spin unitary operation. By using hyperentangled photon pairs, the transmission capacity of the channels can be twice as effective as the normal quantum repeater schemes, which use the photon pairs entangled in only one DOF. The parties in the communication web can link more nodes using the same principle. That is, this method can be used to construct a high-capacity, long-distance quantum repeater in principle. Furthermore, this QD-cavity system can also be realized in an atom-cavity system for the similar relevant

levels [43]. The present scheme has potential applications in various physical systems for the long-distance quantum communication [44–46].

V. DISCUSSION AND CONCLUSION

In this section we discuss the fidelity of using HBSG and HBSA in a promising system with GaAs- or InAs-based QDs in micropillar microcavities. The core component of our protocol is the spin-cavity units whose fidelity and efficiency are discussed briefly in Ref. [39]. In the present hyperentangled-state generation scheme, the spin-cavity unit acts as a SWAP gate, which directly swaps the initial states in the polarization DOF and in the spatial-mode DOF and then records the relationship between the phase information of these two DOFs.

To simplify, we consider the case $|t_0(\omega)| = |r_h(\omega)|$, in which the fidelities to generate (or analysis) $|\phi_{AB}^-\rangle_P \otimes |\phi_{AB}^+\rangle_S$, $|\phi_{AB}^+\rangle_P \otimes |\psi_{AB}^-\rangle_S$, $|\psi_{AB}^+\rangle_P \otimes |\psi_{AB}^-\rangle_S$, and $|\psi_{AB}^-\rangle_P \otimes |\phi_{AB}^+\rangle_S$ can remain unity, whereas the fidelity to generate (or analysis) other 12 hyperentangled Bell states are generally less than one, and depend on the difference between $|t_0|$ and $|r_0|$. The fidelity (in amplitude) is given by

$$\begin{aligned} F_{-+} = F_{+-} = F &= \frac{1}{\sqrt{1+\frac{4(t_0 r_0 + t_h r_h)^2}{r_0^2+t_0^2+r_h^2+t_h^2}}}, \\ F_{++} &= F^2, \quad F_{--} = 1, \end{aligned} \tag{14}$$

Here F_{++}, F_{+-}, F_{-+}, and F_{--} represent the fidelity of the present scheme when the outcomes of the two-spin states are $|++\rangle$, $|+-\rangle$, $|-+\rangle$, and $|--\rangle$, respectively.

The efficiency is

$$\eta = \left[(t_0 r_0 + t_h r_h)^2 + \frac{\left(r_0^2 + t_0^2 + r_h^2 + t_h^2\right)^2}{4}\right]^2. \tag{15}$$

Equation (14) shows that a low κ_s/κ in strong coupling regime is highly required for the present scheme. Figure 5 illustrates the numerical calculations of the fidelity and efficiency of this device vs the coupling strength $g/(\kappa_s + \kappa)$. For large

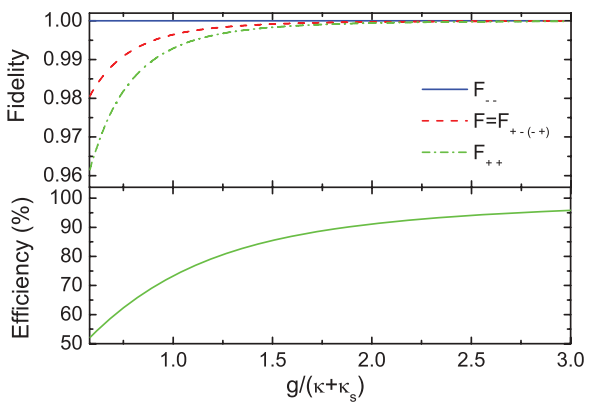

FIG. 5. (Color online) Fidelity and efficiency of the HBSG and HBSA scheme vs the coupling strength $g/(\kappa + \kappa_s)$ when $|t_0| = |r_h|$. F_{++}, F_{+-}, F_{-+}, and F_{--} represent the fidelity of the present scheme when the outcomes of the two-spin states are $|++\rangle$, $|+-\rangle$, $|-+\rangle$, and $|--\rangle$, respectively.

(7.3 μm diameter) micropillar cavities, the strong coupling has been observed in current experiment where the quality factor Q can be improved to $\sim 6.5\times 10^4$, and the corresponding coupling strength is $g/(\kappa_s + \kappa) \simeq 0.8$ [48]. As proposed in Ref. [41], the top mirrors of the high-Q micropillars can be thinned down to obtain a low κ_s/κ. Here we decrease the quality factor to $Q \sim 4.3 \times 10^4$, and set the effective system parameters to be $\kappa_s/\kappa \simeq 0.2$, where the system now with $g/(\kappa + \kappa_s) \simeq 0.58$ remains in the strong coupling regime [47], and the fidelity F can reach 0.98, $F_{++} = 0.96$, with $\eta = 52.2\%$. If we continue to decrease the coupling strength $g/(\kappa_s + \kappa)$ until the spin-cavity unit is regulated into the Purcell (weak-coupling) regime, whereas $g/(\kappa_s + \kappa) \sim 0.49$ and $\kappa_s/\kappa = 0.25$, the corresponding fidelities $F = 0.97$ and $F_{++} = 0.94$, with $\eta = 49.2\%$. The fidelities F_{--} is equal to 1 in both the weak- and strong-coupling regimes. When $g/(\kappa + \kappa_s) = 1.0$, a near-unity fidelity ($F = 0.996, F_{++} = 0.993$, and $F_{--} = 1$) is achievable for the present scheme, with $\eta = 73.3\%$. However, the high efficiencies and high fidelities are achievable only when the side leakage and cavity loss is low in the strong coupling regime.

Given the spin decoherence, the fidelities of the HBSG and HBSA operations decrease by a factor of $F' = [1 + \exp(-t/T)]/2$ [39], where T is the electron-spin coherence time ($\sim\mu$s [49]) and t is the time interval between two photons A and B. t should be considerably shorter than T and longer than $\tau/n_0 \sim$ ns [37], where τ is the cavity photon lifetime and n_0 is the critical photon number of the spin-cavity system [50]. As discussed in Ref. [39], the spin superposition state $|+\rangle$ and $|-\rangle$ can be made from the spin eigenstates by using nanosecond ESR pulses or picosecond optical pulses [50]. The preparation time for the QD-spin superposition state can be significantly shorter than T because of the ultrafast optical coherent control of electron spins in semiconductor quantum wells (femtosecond time scales) and in semiconductor QDs (picosecond time scales) [51]. The photon-spin entanglement enables us to make an ideal quantum nondemolition measurement (QND) of the single spin. After applying a Hadamard gate on the electron spin, the spin superposition states $|+\rangle$ and $|-\rangle$ can be transformed into the spin states $|\uparrow\rangle$ and $|\downarrow\rangle$, respectively, and it can be detected in the $|\uparrow\rangle$ and $|\downarrow\rangle$ basis by measuring the helicity of the transmitted or reflected photon.

In previous Bell-state analysis protocols [16,35,41], the double-sided cavity works as a beam splitter, and transfers a part of the information in the polarization DOF into another DOF or an additional qubit. In the present HBSG and HBSA scheme we exploit the function of the double-sided cavity as a SWAP gate between the polarization Bell states and the spatial-mode Bell states; that is, the states in the polarization DOF and these states in the spatial-mode DOF of the two photons AB can be interchanged. At the same time, the spin in the cavity records the relation of the phase information between these two DOFs.

In summary, we propose a scheme that is used not only to produce photon pairs entangled in both polarization and spatial-mode DOFs but also to completely distinguish the 16 hyperentangled Bell states using the QD-cavity system. By using numerical calculations we prove that the present scheme can both work in the weak- and strong-coupling regimes

within current technology. In the weak coupling regime, the high fidelity and <50% efficiency could be achieved. In the strong coupling regime we expect near-unity fidelity and >52.2% efficiency. This HBSG source and the complete HBSA can be applied as crucial components in high-capacity, long-distance quantum communication, and as an example, we demonstrate how to apply this device in the hyperentanglement quantum repeater. Capable of both generating and analyzing hyperentanglement, the spin-cavity unit can not only work in large-scale quantum communication networks, but also undertake scalable quantum computing and other aspects of quantum information science and technology.

ACKNOWLEDGMENTS

This work was supported by the National Natural Science Foundation of China under Grant No. 11175094, the National Basic Research Program of China under Grants No. 2009CB929402 and No. 2011CB9216002, and the China Postdoctoral Science Foundation under Grant No. 2011M500285.

[1] R. Raussendorf and H. J. Briegel, Phys. Rev. Lett. **86**, 5188 (2001).
[2] C. H. Bennett, G. Brassard, C. Crépeau, R. Jozsa, A. Peres, and W. K. Wootters, Phys. Rev. Lett. **70**, 1895 (1993).
[3] C. H. Bennett and S. J. Wiesner, Phys. Rev. Lett. **69**, 2881 (1992).
[4] A. K. Ekert, Phys. Rev. Lett. **67**, 661 (1991).
[5] P. G. Kwiat, J. Mod. Opt. **44**, 2173 (1997).
[6] J. T. Barreiro, N. K. Langford, N. A. Peters, and P. G. Kwiat, Phys. Rev. Lett. **95**, 260501 (2005).
[7] A. Yabushita and T. Kobayashi, Phys. Rev. A **69**, 013806 (2004).
[8] M. Barbieri, G. Vallone, P. Mataloni, and F. De Martini, Phys. Rev. A **75**, 042317 (2007).
[9] C. Schuck, G. Huber, C. Kurtsiefer, and H. Weinfurter, Phys. Rev. Lett. **96**, 190501 (2006).
[10] J. T. Barreiro, T. C. Wei, and P. G. Kwiat, Nat. Phys. **4**, 282 (2008).
[11] G. Vallone, R. Ceccarelli, F. De Martini, and P. Mataloni, Phys. Rev. A **79**, 030301(R) (2009).
[12] C. Wang, F. G. Deng, Y. S. Li, X. S. Liu, and G. L. Long, Phys. Rev. A **71**, 044305 (2005).
[13] M. M. Wilde and D. B. Uskov, Phys. Rev. A **79**, 022305 (2009).
[14] D. Bruss and C. Macchiavello, Phys. Rev. Lett. **88**, 127901 (2002); N. J. Cerf, M. Bourennane, A. Karlsson, and N. Gisin, *ibid.* **88**, 127902 (2002).
[15] H. J. Briegel, W. Dür, J. I. Cirac, and P. Zoller, Phys. Rev. Lett. **81**, 5932 (1998).
[16] T. J. Wang, S. Y. Song, and G. L. Long, Phys. Rev. A **85**, 062311 (2012).
[17] C. Simon and J. W. Pan, Phys. Rev. Lett. **89**, 257901 (2002); Y. B. Sheng, F. G. Deng, and H. Y. Zhou, Phys. Rev. A **77**, 042308 (2008); Y. B. Sheng and F. G. Deng, *ibid.* **81**, 032307 (2010); **82**, 044305 (2010); X. H. Li, *ibid.* **82**, 044304 (2010); F. G. Deng, *ibid.* **83**, 062316 (2011).
[18] A. Karlsson and M. Bourennane, Phys. Rev. A **58**, 4394 (1998).
[19] F. G. Deng, C. Y. Li, Y. S. Li, H. Y. Zhou, and Y. Wang, Phys. Rev. A **72**, 022338 (2005).
[20] X. S. Liu, G. L. Long, D. M. Tong, and L. Feng, Phys. Rev. A **65**, 022304 (2002).
[21] S. P. Walborn, S. Pádua, and C. H. Monken, Phys. Rev. A **68**, 042313 (2003).
[22] C. Schuck, G. Huber, C. Kurtsiefer, and H. Weinfurter, Phys. Rev. Lett. **96**, 190501 (2006).
[23] M. Barbieri, G. Vallone, P. Mataloni, and F. De Martini, Phys. Rev. A **75**, 042317 (2007).
[24] C. Simon and J. W. Pan, Phys. Rev. Lett. **89**, 257901 (2002).
[25] T.-C. Wei, J. T. Barreiro, and P. G. Kwiat, Phys. Rev. A **75**, 060305(R) (2007).
[26] Y. B. Sheng, F. G. Deng, and G. L. Long, Phys. Rev. A **82**, 032318 (2010).
[27] J. H. Shapiro, Phys. Rev. A **73**, 062305 (2006).
[28] J. Gea-Banacloche, Phys. Rev. A **81**, 043823 (2010).
[29] T. Calarco, A. Datta, P. Fedichev, E. Pazy, and P. Zoller, Phys. Rev. A **68**, 012310 (2003).
[30] V. Zwiller, T. Aichele, F. Hatami, W. T. Masselink, and O. Benson, Appl. Phys. Lett. **86**, 091911 (2005).
[31] O. Benson, C. Santori, M. Pelton, and Y. Yamamoto, Phys. Rev. Lett. **84**, 2513 (2000).
[32] G. Chen, C. F. Li, Z. Q. Yin, Y. Zou, L. X. He, and G. C. Guo, Europhys. Lett. **89**, 44002 (2010).
[33] A. Aufféves-Garnier, C. Simon, J. M. Gérard, and J. P. Poizat, Phys. Rev. A **75**, 053823 (2007).
[34] E. Waks and J. Vuckovic, Phys. Rev. Lett. **96**, 153601 (2006).
[35] C. Bonato, F. Haupt, S. S. R. Oemrawsingh, J. Gudat, D. P. Ding, M. P. van Exter, and D. Bouwmeester, Phys. Rev. Lett. **104**, 160503 (2010).
[36] C. Y. Hu, A. Young, J. L. O'Brien, W. J. Munro, and J. G. Rarity, Phys. Rev. B **78**, 085307 (2008).
[37] C. Y. Hu, W. J. Munro, and J. G. Rarity, Phys. Rev. B **78**, 125318 (2008).
[38] A. M. Stephens, Z. W. E. Evans, S. J. Devitt, A. D. Greentree, A. G. Fowler, W. J. Munro, J. L. O'Brien, K. Nemoto, and L. C. L. Hollenberg, Phys. Rev. A **78**, 032318 (2008).
[39] C. Y. Hu, W. J. Munro, J. L. O'Brien, and J. G. Rarity, Phys. Rev. B **80**, 205326 (2009).
[40] C. Wang, Y. Zhang, and G. S. Jin, Phys. Rev. A **84**, 032307 (2011).
[41] C. Y. Hu and J. G. Rarity, Phys. Rev. B **83**, 115303 (2011).
[42] A deterministic and nondestructive parity check gate can be built for the spin entangled states (see Ref. [40]). It can be used for entanglement purification. Therefore, the spin-cavity unit can work as a full hyperentanglement quantum repeater (see Ref. [15]) that combines entanglement generation, entanglement swapping, entanglement purification, and quantum memory. Quantum communications over arbitrary long distance are possible with hyperentanglement quantum repeaters by using this device.
[43] K. Koshino, S. Ishizaka, and Y. Nakamura, Phys. Rev. A **82**, 010301(R) (2010).

[44] T. Schmitt-Manderbach, H. Weier, M. Fürst, R. Ursin, F. Tiefenbacher, T. Scheidl, J. Perdigues, Z. Sodnik, C. Kurtsiefer, J. G. Rarity, A. Zeilinger, and H. Weinfurter, Phys. Rev. Lett. **98**, 010504 (2007).

[45] A. Fedrizzi, R. Ursin, T. Herbst, M. Nespoli, R. Prevede, T. Scheidl, F. Tiefenbacher, T. Jennewein, and A. Zeilinger, Nat. Phys. **5**, 389 (2009).

[46] X. M. Jin, J. G. Ren, B. Yang, Z. H. Yi, F. Zhou, X. F. Xu, S. K. Wang, D. Yang, Y. F. Hu, S. Jiang, T. Yang, H. Yin, K. Chen, C. Z. Peng, and J. W. Pan, Nat. Photon. **4**, 376 (2010).

[47] Here g and κ can be controlled independently as g is determined by the trion oscillator strength and the cavity modal volume, whereas κ by the cavity quality factor only [41].

[48] V. Loo, L. Lanco, A. Lemaître, I. Sagnes, O. Krebs, P. Voisin, and P. Senellart, Appl. Phys. Lett. **97**, 241110 (2010).

[49] J. R. Petta, A. C. Johnson, J. M. Taylor, E. A. Laird, A. Yacoby, M. D. Lukin, C. M. Marcus, M. P. Hanson, and A. C. Gossard, Science **309**, 2180 (2005); A. Greilich, D. R. Yakovlev, A. Shabaev, Al. L. Efros, I. A. Yugova, R. Oulton, V. Stavarache, D. Reuter, A. Wieck, and M. Bayer, *ibid.* **313**, 341 (2006); M. Kroutvar, Y. Ducommun, D. Heiss, M. Bichler, D. Schuh, G. Abstreiter, and J. J. Finley, *ibid.* **432**, 81 (2004); R. Ursin *et al.*, Nature (London) **3**, 481 (2007).

[50] H. J. Kimble, in *Cavity Quantum Electrodynamics*, edited by P. Berman (Academic, San Diego, 1994).

[51] J. A. Gupta, R. Knobel, N. Samarth, and D. D. Awschalom, Science **292**, 2458 (2001); P. C. Chen, C. Piermarocchi, L. J. Sham, D. Gammon, and D. G. Steel, Phys. Rev. B **69**, 075320 (2004); J. Berezovsky, M. H. Mikkelsen, N. G. Stoltz, L. A. Coldren, and D. D. Awschalom, Science **320**, 349 (2008).